Journal of Engineering and Applied Sciences 12 (16): 4016-4021, 2017
ISSN: 1816-949X

Large Effective Area Square Photonic Crystal Fiber for Optical Communications

[1]Feroza Begum, [1]Abul Kalam Azad, [1]Saifullah Abu Bakar, [1]Iskander Petra,
[2]Kazuya Miyagi and [2]Yoshinori Namihira
[1]Faculty of Integrated Technology, Universiti Brunei Darussalam,
1410 Gadong BE, Brunei Darussalam
[2]Graduate School of Engineering and Science, University of the Ryukyus, 903-0213 Okinawa, Japan

Abstract: This study presents a large effective area square photonic crystal fiber for optical communication systems. In order to achieve large effective area, a five rings square photonic crystal fiber with missing first ring air holes is proposed. The designed PCF represents that it is possible to obtain large effective area, better chromatic dispersion, low confinement losses and near zero splice loss in the entire telecommunication band by using modest number of design parameters based on full vector finite-difference method. Additionally, the effect of bending on confinement losses of the proposed square photonic crystal fiber has been investigated.

Key words: Photonic crystal fiber, chromatic dispersion, effective area, splice loss, telecommunication, investigated

INTRODUCTION

Photonic Crystal Fibers (PCFs), optoelectronic devices and systems have enabled rapid progress in telecommunications in recent decades (Knight *et al*., 1996; Begum *et al*., 2007). As optical fiber technology advances, fibers are becoming thinner, stronger, lighter and more flexible. Now a days, optically-driven data exchange media are playing a central role in many new applications such as defense, security, sensing, transportation, computing and medicine. Future usage of optical fibers extends into special communications applications through the exploitation of multi-gigabit rates, low-cost and low-loss fibers and other physical and optical characteristics of these waveguides. One emerging technology in this sector is Fiber To The Home (FTTH), also called Fiber To The Premises (FTTP) or Fiber To The Building (FTTB). FTTH brings fiber optics directly to homes/buildings while a similar technology, Fiber To The Node (FTTN), brings the fiber optics to a community and then connects the fiber optics to the homes with a traditional copper cable. In the past, consumer telecom networks had a high-speed backbone with lower speed cables running to user's homes and offices. The high-speed backbones were able to carry the combined capacity of all the users but the infrastructure running to the users severely limited the speed and bandwidth available to consumers. FTTH allows for much larger bandwidth and much faster delivery speeds which are essential for modern "triple-play" deliveries in which access providers offer video, data and telephony services. It also requires the installation of new transmission, wiring and receiving infrastructure. Both the increase in number of channel and the data rate per channel implies increasing the power level in the fiber. The very large effective area enables high power levels without nonlinear effects or material damage.

PCFs present great potential as transmission fibers. One of the benefits is the possibility to design single-mode pure-silica core fibers with large effective areas (Birks *et al*., 1997) hence alleviating nonlinear impairments. In optical transmission systems, fiber confinement loss is a very important parameter. Recent progress in fabrication technology has allowed for the reduction of the transmission loss down to a current record value of 0.2 dB/km at 1550 nm (Begum *et al*., 2009; Roberts *et al*., 2005) as well as the drawing of longer fibers with uniform structural properties. Therefore, the time has come to explore the use of PCFs for transmission applications. So far several large effective area PCFs with remarkable dispersion and leakage properties have been reported (Matsui *et al*., 2005; Reeves *et al*., 2002; Florous *et al*., 2006; Tsuchida *et al*., 2005; Rostami and Soofi, 2011; Ademgil and Haxha, 2012; Soriano *et al*., 2015). Reference (Matsui *et al*., 2005) have theoretically achieved large effective area >100 μm^2 using a double cladding structure with two different pitch and air hole diameters. A double cladding PCF sets a challenge on the fabrication issue. Reeves *et al*. (2002), Rostami and Soofi (2011) have realized PCFs with effective area 44 μm^2 but

Corresponding Author: Feroza Begum, Faculty of Integrated Technology, Universiti Brunei Darussalam, 1410 Gadong BE, Brunei Darussalam

the PCF has a high confinement loss and 11 air hole rings and >80 μm^2 with 11 air hole rings defected core PCFs, respectively. Moreover (Florous *et al*., 2006; Tsuchida *et al*., 2005; Ademgil and Haxha, 2012) have contained arbitrary chosen defected air holes, Germanium doped core and higher index rod in the cladding region, respectively those are also difficult to fabricate. Furthermore, Soriano *et al*. (2015) have designed Sierpinski fractal PCF with effective area around 270 μm^2 at 1.55 μm wavelength which will face also fabrication issue. Based on current knowledge, it is evident that continuing research in all the related technologies is needed to improve the structure, cost and performance targets of both present and future fiber implementations. We explore the possibility of designing a large mode area photonic crystal fiber with low confinement losses using the square PCF by eliminating the first air hole ring and modulating the diameter of second and third air hole rings. The large mode area PCFs are used in many applications such as fiber lasers, attenuation of nonlinear effects and high power density. It is possible to get large mode area from the proposed square PCFs which allowing to decrease the values of the nonlinear parameters of the fiber.

In this study, we present a large effective area Square PCFs (SPCFs) with only 5 air hole rings in the entire S+C+L telecommunication band (1.46-1.625) by using full-vector Finite Difference Method (FDM) (Begum *et al*., 2009; Shen *et al*., 2003). From the numerical simulation results, it is found that it is possible to obtain larger effective area of 410 μm^2 at 1.55 μm wavelength, better chromatic dispersion, low confinement loss and reasonable splice loss in the entire telecommunication band. This proposed square PCF may pave the way for the next generation high speed data transmission systems.

MATERIALS AND METHODS

Theory of calculation: For the numerical simulations we employed a full-vector Finite Difference Method (FDM) with anisotropic Perfectly Matched Layers (PMLs) (Begum *et al*., 2009; Shen *et al*., 2003; Begum and Namihira, 2012). The PML is strongly absorbs outgoing waves from the interior of a computational region without reflecting them back into the interior. The base material of the proposed SPCFs is pure silica which refractive index is considered here 1.45. It is possible to calculate different properties of PCF such as chromatic dispersion D(λ), confinement loss LC and effective area Aeff by using FDM. These parameters are calculated by the following equations.

Chromatic dispersion, D(λ): The material dispersion given by Sellmeier equation is directly included in the calculation. Therefore, in this calculation, chromatic dispersion corresponds to the total dispersion of PCF (Begum *et al*., 2009; Shen *et al*., 2003; Begum and Namihira, 2012):

$$D(\lambda) = -\frac{\lambda}{c}\frac{d^2\,\mathrm{Re}[n_{eff}]}{d\lambda^2} \tag{1}$$

Where:

λ = The operating wavelength in μm
c = The velocity of light in a vacuum
$\mathrm{Re}[n_{eff}]$ = The real part of the effective index derived by solving Maxwell's equations

Effective area, A_{eff}: The effective area is an important quantity in the understanding of nonlinear phenomena in PCFs. It was originally introduced as a measure of nonlinearities, a large effective area gives a low density of power needed for low nonlinear effect. The effective area and the nonlinear properties can be calculated by using following equation (Begum *et al*., 2009; Shen *et al*., 2003; Begum and Namihira, 2012):

$$A_{eff} = \frac{\left(\int_{-\infty}^{\infty}\int_{-\infty}^{\infty}|E|^2\,dxdy\right)^2}{\int_{-\infty}^{\infty}\int_{-\infty}^{\infty}|E|^4\,dxdy} \tag{2}$$

$$\gamma = \frac{n_2 w}{cA_{eff}} = \frac{2\pi n_2}{\lambda A_{eff}} \tag{3}$$

However, the effective area is related to the Gaussian function Mode Field Diameter (MFD), i.e., spot size:

$$A_{eff} = \pi w^2 \tag{4}$$

Where:

E = The electric field
w = The spot size
n_2 = The non-linear refractive index coefficient in the non-linear part of the refractive index
λ = The non-linear property

So, it would be desirable to achieved large effective area to diminish the non-linear effect.

Confinement loss L_c: The confinement loss of the fundamental mode is calculated from the imaginary part of the effective index using the following equation (Begum *et al*., 2009; Shen *et al*., 2003; Begum and Namihira, 2012):

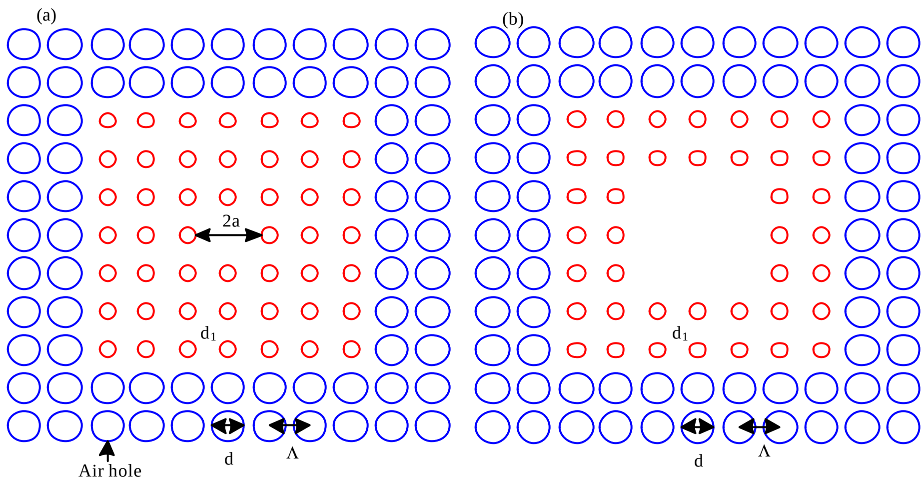

Fig. 1: PCF structure: a) With first air hole ring and b) Without first air hole ring which is the proposed square PCF

$$L_c = -20\log_{10} e^{-k_0 \operatorname{Im}[n_{eff}]} = 8.686 k_0 \operatorname{Im}[n_{eff}] \quad (5)$$

Where:

k_0 = The propagation constant in free space

Im (n_{eff}) = The imaginary part of the complex effective index n_{eff}

Splice loss L_S: Optical power loss at the splicing point of two ends of optical fiber is known as splice loss. The splice loss is a very important to design consideration for Single Mode Fiber (SMF). When coupling two similar fibers or a PCFs with SMF using the splicing techniques, a mismatch occurs due to the dissimilar Mode Field Diameter (MFD) or geometrical misalignments during the fusion process that leads losses known as the splice loss. The optical field distribution of the fundamental mode in PCFs has been approximated by using the ITU-T Petermann II definition. Here, ITU-T is the international telecommunication union-telecommunication standardization sector. The splicing losses can be calculated by the following equation (Saval *et al*., 2005):

$$L_s = -20\log_{10}\left[\frac{2(w_{SMF} w_{PCF})}{w_{SMF}^2 + w_{PCF}^2}\right] \quad (6)$$

where, w_{SMF} and w_{PCF} are the MFD of the SMF and PCF, respectively.

Structure of the proposed PCF: In this study, we consider a square PCFs having a solid core surrounded by five air hole rings running along the fiber axis as shown in Fig. 1a where d_1 and d are the diameters in the small and large air hole rings, respectively, Λ is the air hole pitch and 2a is the core diameter. The proposed structure is shown in Fig. 1b and in this structure the first air hole rings are omit, second and third air hole rings diameters are d_1 and the diameters of the remaining air holes remain the same d. It should be noted that host material is pure silica. In conventional PCFs (the ones with same air hole diameters in the cladding region) it is difficult to control optical properties such as dispersion and dispersion slope simultaneously in a broad wavelength range. Therefore, in our design we reduced the air hole diameter d_1 for the second and third rings. On the other hand, large size of air hole d is chosen in order to give better field confinement of guided mode and hence low confinement loss.

RESULTS AND DISCUSSION

Effective area: Figure 2a demonstrates the wavelength dependence properties of optimum effective area for the 5-rings PCFs in Fig. 1 where d_1 = 0.4 μm, d = 2.8 μm for a fixed pitch Λ = 4.0 μm. From Fig. 2a, it is found that the effective area is around 410 μm^2 at 1.55 μm wavelength. Figure 2b represents the wavelength dependence properties of effective area for air hole diameter of different rings with the optimum one. The optimum effective area curve is express by the straight line (red line). It is seen that the effective area is 400 μm^2 for the four rings in 1.3-1.7 μm wavelength range. The effective area curve (dash line) is shown after increasing only the second and third ring air hole diameter d_1 from 0.4-1.2 μm to keep the rest of the parameters remain same. It is found that the effective area is <50 μm^2 in the entire wavelength range. The effective area curve (dot line) is shown when all the air hole diameters are equal in size where d_1 = d = 2.8 μm, Λ = 4.0 μm. It is observed that the effective area is not >20 μm^2 in the whole wavelength

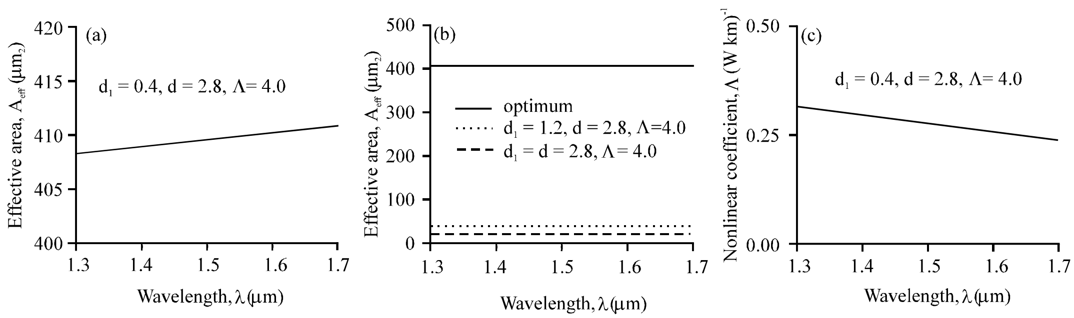

Fig. 2: a) Effective area of the proposed SPCF without first air hole ring as a function of wavelength; b) Effective area comparison and c) Non-linear coefficient of the proposed PCF without first air hole ring for different parameters with optimum one as a function of wavelength

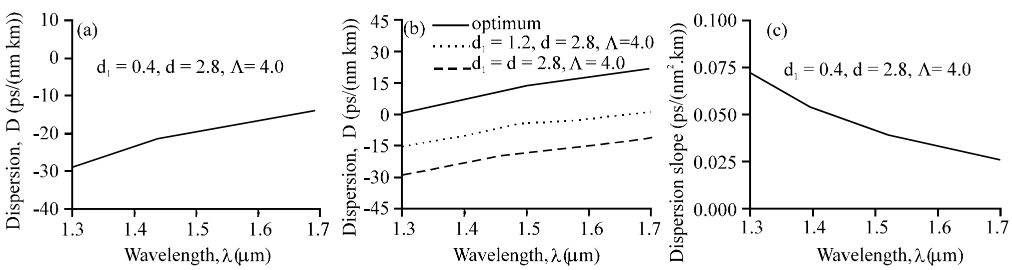

Fig. 3: a) Chromatic dispersion property of the proposed square PCFs without first air hole ring as a function of wavelength; b) Chromatic dispersion comparison of the proposed square PCFs without first air hole ring for different parameters with optimum one as a function of wavelength and c) Chromatic dispersion slop of the proposed square PCFs as a function of wavelength

range. From this graph, it is concluded that the effective area of this proposed square PCFs is greatly influenced by the diameter of the first and second air hole ring. From Fig. 2a and b, it is observed that effective area increases with increasing operating wavelengths and it is the usual characteristics of effective area. It means that optical power density decreases with increasing values of wavelength. The large mode area enables high power levels and this high power to be transmitted through the optical fiber without nonlinear effects or material damage. Figure 2c shows the wavelength dependence non-linear coefficient property of the proposed square PCFs for the optimum parameters d_1 = 0.4 μm, d = 2.8 μm and Λ = 4.0 μm. From this graph, it has been seen that the nonlinear coefficient decreases with increasing wavelength and this mean that larger the effective area, A_{eff} lesser the optical power density which lead low non-linearity. The nonlinear coefficient is 0.26 (W.km^{-1}) at 1.55 μm wavelength for d_1 = 0.4 μm, d = 2.8 μm and Λ = 4.0 μm of the proposed square PCF.

Chromatic dispersion: Figure 3a demonstrates the wavelength dependence properties of chromatic dispersion for the 5-rings PCFs in Fig. 1 where d_1 = 0.4 μm, d = 2.8 μm for a fixed pitch Λ = 4.0 μm. From Fig. 3a, it is found that the wavelength range the proposed PCFs is owning chromatic dispersion -15.8 ps/(nm.km) at 1.55 μm wavelength. Fig. 3b depicts the influence of variations in the air hole diameters with fixed pitch Λ for the proposed fiber cladding on the dispersion behavior. In Fig. 3b, the dashed line shows the effect of changing diameter d_1 = 1.2 μm (second and third rings) and d = 2.8 μm (fourth and fifth rings) on the chromatic dispersion. Here all the other parameters are also kept to be constant. At the operating wavelength 1550 nm, the peak value of the negative dispersion decreases with increasing the air hole diameters. In this graph, the chromatic dispersion value is -2.7 ps/(nm km) at 1.55 μm wavelength. Furthermore, in Fig. 3b, the dotted line shows the effect of changing diameter d_1 = 2.8 μm (second and third rings), d = 2.8 μm of the fourth and fifth rings and Λ = 4.0 μm on the chromatic dispersion. The simulation results depicts that the peak value of the chromatic dispersion shifts with increasing d_1 and d. In this plot, the chromatic dispersion value is 15.7 ps/(nm.km) at 1.55 μm wavelength. According to simulation, it has been seen that chromatic dispersion is greatly depend on the air hole diameter d_1. Figure 3c represents the dispersion slope as a function

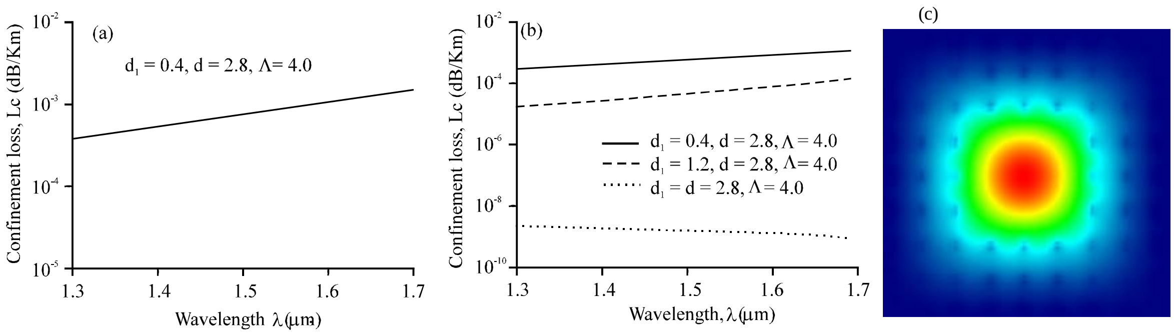

Fig. 4: a) Confinement loss property of the proposed square PCFs without first air hole ring as a function of wavelength; b) Confinement loss comparison of the proposed square PCFs without first air hole ring for different parameters with optimum one as a function of wavelength and c) Optical field of the proposed square PCFs without first air hole ring

slope as a function of wavelength for optimum parameters d_1 = 0.4 µm, d = 2.8 µm and pitch Λ = 4.0 µm. From this graph, it has been seen that the dispersion slop decreases with increasing the wavelength. The dispersion slope varies from 0.025-0.075 ps/(nm^2.km) in the wavelength range of 1.3-1.7 µm.

Confinement loss: Figure 4a depicts the wavelength dependence properties of confinement loss for the 5-rings PCF in Fig. 1 where d_1 = 0.4 µm, d = 2.8 µm for a fixed pitch Λ = 4.0 µm. From Fig. 4a, it is found that the confinement loss is <10^{-2} dB/km in the wavelength range of 1.3-1.7 µm. The present large value of d is selected for better field confinement. Because the confinement losses strongly depend on the number of air hole rings, air hole diameters and air hole spacing. Figure 4b represents the effect of variations in the air hole diameters with fixed pitch Λ for the proposed square PCFs on the confinement loss. In Fig. 4b, the dashed line shows the effect of changing diameter d_1 = 1.2 µm (second and third rings) and d = 2.8 µm (fourth and fifth rings) on the confinement loss. Here other parameters pitch Λ = 4.0 µm is kept constant. From this graph, it is seen that the value of the confinement loss decreases with increasing the air hole diameters in the entire wavelength region. The value of confinement loss is almost <10^{-4} dB/km in the entire wavelength range for the parameters d_1 = 1.2, d = 2.8 µm and Λ = 4.0 µm. Furthermore, in Fig. 4b, the dotted line shows the influence of changing diameter d_1 = 2.8 µm (second and third rings), d = 2.8 µm of the fourth and fifth rings and Λ = 4.0 µm on the confinement loss. The simulation results depicts that the value of the confinement loss decreases more with increasing d_1 and d. The value of confinement loss is almost <10^{-8} dB/km for the parameters d_1 = d = 2.8 µm and Λ = 4.0 µm. Moreover it has been seen that the dash line (d_1 = 1.2 µm, d = 2.8 µm and Λ = 4.0 µm) and dot line (d_1 = d = 2.8 µm and Λ = 4.0 µm) confinement losses are lower than optimum one (d_1 = 0.4 µm, d = 2.8 µm and Λ = 4.0 µm). According to simulation result, it has been seen that confinement loss is greatly depend on the air hole diameter d_1. Figure 4c shows the optical field distribution of the proposed PCFs. From this figure it is seen that the optical field spread over the entire core and gives rise to the effective area.

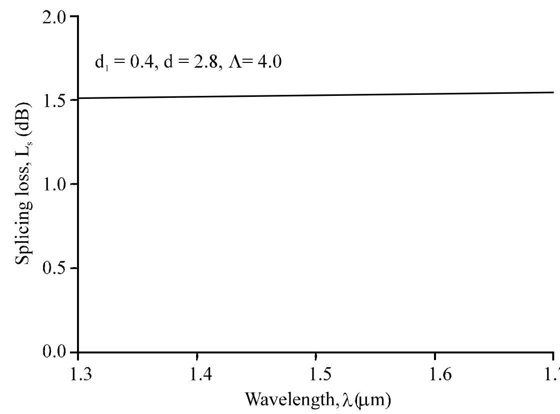

Fig. 5: Calculated splice loss between conventional fiber and proposed square PCFs without first air hole ring as a function of wavelength

Splice loss: Figure 5 shows the splice losses between the proposed square PCFs and conventional SMF with two defected rings. It should be pointed out that the MFD of the SMF is considered 10.8 µm for this calculation. Using an FDM model we have numerically determined the splice loss for SMF to PCF splices over a range of parameters. It is seen from the figure that the splice losses are around 1.5 dB in all wavelengths. Low fusion splice loss is important for successful, low cost cable installations and growth to faster networks. Recently the new fiber connecting technique is demonstrated therefore the splicing loss may not be important issue (Saval *et al.*, 2005).

Thus, we have observed that it is possible to design large effective area square PCFs without first air hole ring. On the other hand, the proposed square PCFs has flattened dispersion in a wavelength range of 1.3-1.7 μm with very low confinement loss, better splice loss and a modest number of design parameter. Therefore, the large effective area PCFs has the potential to lead a crucial role in future all optical reconfigurable high speed transmission applications.

CONCLUSION

We have proposed and demonstrated a square PCF which is applicable to FTTH optical communication applications for the next generation communications. It has been shown through numerical results that it is possible to design a large effective area square PCFs with a chromatic dispersion of -15.8 ps/(nm.km), a confinement loss below 0.0008 dB/km, effective area of 410 μm^2, low nonlinear coefficient of 0.26 $(W.km^{-1})$ at 1.55 μm wavelength and splice loss below 1.5 dB, at 1.55 μm wavelength, respectively, by appropriate choosing the core radius, the hole pitch and the air hole diameters. From the design point of view, the main advantage of the proposed square PCFs is that it is possible to achieve large effective area with low confinement loss only using modest number of design parameters.

REFERENCES

Ademgil, H. and S. Haxha, 2012. Endlessly single mode photonic crystal fiber with improved effective mode area. Opt. Commun., 285: 1514-1518.

Begum, F. and Y. Namihira, 2012. Photonic Crystal Fiber for Medical Applications. University of the Ryukyus, Nishihara, Japan,.

Begum, F., Y. Namihira, S.A. Razzak, S. Kaijage and N.H. Hai *et al.*, 2009. Design and analysis of novel highly nonlinear photonic crystal fibers with ultra-flattened chromatic dispersion. Opt. Commun., 282: 1416-1421.

Begum, F., Y. Namihira, S.M.A. Razzak, S. Kaijage and K. Miyagi *et al.*, 2007. Highly nonlinear dispersion-flattened square photonic crystal fibers with low confinement losses. Opt. Rev., 14: 120-124.

Begum, F., Y. Namihira, S.M.A. Razzak, S. Kaijage and N.H. Hai et al., 2009. Novel broadband dispersion compensating photonic crystal fibers: Applications in high speed transmission systems. Opt. Laser Technol., 41: 679-686.

Birks, T.A., J.C. Knight and P.S.J. Russell, 1997. Endlessly single-mode photonic crystal fiber. Opt. Lett., 22: 961-963.

Florous, N., K. Saitoh and M. Koshiba, 2006. The role of artificial defects for engineering large effective mode area, flat chromatic dispersion and low leakage losses in photonic crystal fibers: Towards high speed reconfigurable transmission platforms. Opt. Express, 14: 901-913.

Knight, J.C., T.A. Birks, P.S.J. Russell and D.M. Atkin, 1996. All-silica single-mode optical fiber with photonic crystal cladding. Opt. Lett., 21: 1547-1549.

Matsui, T., J. Zhou, K. Nakajima and I. Sankawa, 2005. Dispersion-flattened photonic crystal fiber with large effective area and low confinement loss. J. Lightwave Technol., 23: 4178-4183.

Reeves, W.H., J.C. Knight, P.S.J. Russell and P.J. Roberts, 2002. Demonstration of ultra-flattened dispersion in photonic crystal fibers. Opt. Express, 10: 609-613.

Roberts, P.J., F. Couny, H. Sabert, B.J. Mangan and D.P. Williams et al., 2005. Ultimate low loss of hollow-core photonic crystal fibres. Opt. Express, 13: 236-244.

Rostami, A. and H. Soofi, 2011. Correspondence between effective mode area and dispersion variations in defected core photonic crystal fibers. J. Lightwave Technol., 29: 234-241.

Saval, L.S.G., T.A. Birks, N.Y. Joly, A.K. George and W.J. Wadsworth et al., 2005. Splice-free interfacing of photonic crystal fibers. Opt. Lett., 30: 1629-1631.

Shen, L.P., W.P. Huang and S.S. Jian, 2003. Design of photonic crystal fibers for dispersion-related applications. J. Lightwave Technol., 21: 1644-1651.

Soriano, A.D., O.A. Mora and A. Dengra, 2015. A new low-dispersion and large-effective-area PCF based on a fractal design. Opt. Fiber Technol., 21: 69-72.

Tsuchida, Y., K. Saitoh and M. Koshiba, 2005. Design and characterization of single-mode holey fibers with low bending losses. Opt. Express, 13: 4770-4779.